Studying chaotic systems using microcomputer simulations and Lyapunov exponents

Sergio De Souza-Machado[a)]
Physics Department, The College of Wooster, Wooster, Ohio 44691

R. W. Rollins
Department of Physics and Astronomy, Ohio University, Athens, Ohio 45701

D. T. Jacobs and J. L. Hartman
The College of Wooster, Wooster, Ohio 44691

(Received 10 February 1989; accepted for publication 16 May 1989)

The study of nonlinear systems in an undergraduate setting has become important, and this article describes the use of an interactive simulation in introducing students to the new techniques used to characterize deterministic chaos. Lyapunov exponents are introduced with emphasis on their physical significance. The results of numerical experiments on the driven, damped, Duffing two-well oscillator are reported and the global behavior of the Lyapunov exponent spectra is presented. The results confirm an important sum rule satisfied by the Lyapunov exponent spectra. Interesting, structured behavior of the Lyapunov exponent spectra is observed as the Duffing oscillator system follows the period-doubling route to chaos.

I. INTRODUCTION

Most of the physical systems studied at the undergraduate level display regular, predictable behavior. The systems are usually modeled by *linear* differential equations, which can eventually be solved analytically to give a closed-form solution expressible in terms of elementary functions (trigonometric, polynomial, exponential, etc.). These systems are *deterministic*, since their future behavior is completely described by a given set of initial conditions and the modeling equations. And the physical solutions are clearly *predictable* for long times. (The unstable solutions that "blow up" for linear systems are "nonphysical" and usually are not considered further.) It is important to realize that such regular motion holds for only a small number of idealized physical systems.

On the other hand, real systems almost always must be described by *nonlinear* equations. These equations are, under reasonable conditions of "smoothness," also *deterministic* (i.e., a set of initial conditions determines a unique solution for all time). However, it is now clear that nonlinear deterministic systems typically behave in such a way that, even with the most powerful computers available, it would be impossible to predict their state for a very long time. This interesting, and apparently contradictory, behavior (*deterministic* yet *unpredictable*) is possible because the solutions for a nonlinear system can depend very sensitively on the initial conditions. In effect, the nonlinearity can prevent solutions that have an instability from blowing up; hence, these unstable solutions remain physically observable for all time. Furthermore, it is usually not possible to use analytical techniques to find the solution in a closed form. Examples of such systems are usually not mentioned at the undergraduate level. This often leaves students with the mistaken idea that all systems are modeled by linear equations that can be solved in closed form, and, perhaps a more serious misconception, that given an initial condition with finite precision, the state of any classical system can be predicted with about the same precision for a long time.

In the past, the general understanding was that classical systems could be unpredictable only if they were influenced by some random internal or external force (no longer deterministic), or had so many degrees of freedom as to make the system so complex that predictions were impracticable. (Each degree of freedom requires a pair of phase-space coordinates, such as position–velocity, to describe the dynamic state of the system.) But recent studies have shown that many nonlinear systems that are deterministic and have only a few degrees of freedom are, nevertheless, unpredictable under typical conditions. In fact, the number of degrees of freedom need only be greater than 1. The study of the global behavior of such nonlinear systems has recently been called the study of *Chaos* and the solutions that have sensitive dependence on initial conditions are called *chaotic*. (The word chaos was first prominently used in this connection in 1975 by Tien-Yien Li and James Yorke in a paper entitled "Period Three Implies Chaos."[1]) The general public has been made more aware of the recent advances in the field of Chaos by the best-selling book of that title by James Gleick.[2] For the scientist or mathematician, several introductory books on chaos and nonlinear dynamics are now available,[3–8] and there are at least two books containing reprints of important papers in the field.[9] Also highly recommended is the set of books by Abraham and Shaw,[10] which contain many delightful figures that are very helpful in gaining a physical picture of the global behavior and the structure of chaotic solutions in three-dimensional phase space. Finally, as this paper attempts to demonstrate clearly, the microcomputer is a very useful tool for studying and experimenting in the new field of chaos.

The computer plays an important role in the study of chaotic systems, since the nonlinear modeling equations cannot be solved to give a closed-form solution. Numerical techniques are used to study solutions represented by a trajectory through phase space, starting from a particular initial condition. Chaotic behavior is not exhibited for all parameter values in the model equations (parameters could be the amplitude and frequency of a driving force, damping strength, etc.). Rather, the system is predictable for one set of parameter values, and chaotic (unpredictable) for another set. Furthermore, numerical studies have shown that, although the solutions can be chaotic, there is a great deal of order, or structure, to deterministic chaos. The dis-

covery that many systems exhibit universal scaling laws at the transition to chaos was very important. These universal scaling laws are roughly similar in significance within nonlinear dynamics as simple harmonic motion is in linear dynamics. Several new quantitative techniques have been developed to determine whether a particular trajectory (solution) is chaotic, and, if so, to give a quantitative measure of how chaotic it is. These techniques include determining the fractal dimension of those points of phase space traversed by a chaotic trajectory during a very long (ideally infinite) time interval, and determining the Lyapunov exponents that measure how rapidly two nearby (ideally infinitesimally close) trajectories separate from one another in phase space.[3-9]

Many biological, chemical, and physical systems have been found to exhibit chaotic behavior.[3-9] Deterministic chaos seems to be everywhere, and it is important to introduce undergraduate students to nonlinear dynamics and the current methods used to study chaos. There have been several recent articles in this Journal detailing undergraduate experiments on physical systems that demonstrate some aspects of chaotic behavior.[11] In this article we discuss the results of *numerical experiments*, carried out on a microcomputer, on simple nonlinear equations modeling physical systems. The work was part of a senior independent study project of one of the authors (SDS-M). The use of such numerical experimentation has been, and will continue to be, crucial in the development of the field of chaos. In particular, we will discuss the calculation and interpretation of Lyapunov exponents as an indicator that a system is chaotic and how chaotic it is. We present extensive results on the Duffing two-well oscillator and briefly discuss results obtained on two other classic chaotic systems: the Lorenz system and a driven Van der Pol oscillator. All results discussed were obtained on common, relatively inexpensive personal computers. Before presenting the results, we will briefly discuss the concept of attractors in phase space for dissipative systems, some of the universal routes by which systems can become chaotic, and the definition and physical significance of Lyapunov exponents.

II. DISSIPATIVE SYSTEMS AND ATTRACTORS

We will focus our attention on deterministic systems modeled by coupled, nonlinear, first-order, ordinary differential equations of the form

$$\frac{d\mathbf{X}}{dt} = \mathbf{G}(\mathbf{X},\mathbf{L}), \tag{1}$$

where $\mathbf{X}$ is the phase-space vector $(X_1,...,X_n)$, the X_i are phase-space coordinates, $\mathbf{L}$ is a set of parameters $L_1,...,L_m$, $\mathbf{G}$ is a vector function, and n is the phase-space dimension. The set of differential equations is said to be autonomous when $\mathbf{G}$ does not depend explicitly on the time t. Equation (1) determines the set of solution curves, $\mathbf{X}(t)$ (trajectories), called the *flow* in phase space. The vector function $\mathbf{G}$ is called the generalized velocity vector field associated with the flow. In this article, we refer to the points in phase space moving along the solution curves as the action of the flow.

The systems considered in this article are dissipative due to the presence of internal frictionlike terms. The flow along trajectories in phase space, for dissipative systems of this type, is such that the volume of an arbitrary droplet of initial conditions in phase space will contract as the flow progresses in time. The rate of change of these volume elements, dV/dt, is given by the following expression[12]:

$$\frac{dV}{dt} = \int\int_v \cdots \int \left(\sum_{i=1}^{n} \frac{\partial G_i}{\partial X_i} \right) dX_1 \cdots dX_n, \tag{2}$$

where $dX_i/dt = G_i$, n is the dimension of the embedding phase space, and the summation term is the generalized divergence of $\mathbf{G}$ also called the Lie derivative.[12] Dissipative systems are defined by $dV/dt < 0$. Dissipative systems are to be distinguished from conservative (or Hamiltonian) systems where Eq. (1) are Hamilton's equations, which obey Liouville's theorem (i.e., $dV/dt = 0$). A brief review of conservative systems recently appeared by Chernikov *et al.*[13]

Any trajectory of a *dissipative* system as $t \to \infty$ will approach a bounded region of phase space called an *attractor*. Since all the trajectories with initial conditions in a phase-space volume V end up on an attractor as $t \to \infty$, and since $dV/dt < 0$, then the volume of phase space occupied by the attractor is 0. Hence, the dimension of the attractor will be less than the dimension of the full phase space. An example is the case of an unforced damped simple pendulum that eventually comes to rest: the attractor being the fixed point (0,0) in the angular position–angular velocity phase plane. Other types of attractors are limit cycle and torus attractors.[3-10] The dimensions of these three attractors are integral numbers: 0 for the fixed point; 1 for the limit cycle; and 2 (or 3, etc., depending on the type) for the torus. For these three types of attractors, the separation of two trajectories, which are near the attractor and initially very close to each other, does not increase with time, and the evolution of the system remains predictable.[14]

It has been found that, in the case of nonlinear systems exhibiting chaos, the separation of two nearby trajectories increases *exponentially* with time. Consider two initial conditions in phase space, $\mathbf{X}_0$ and $(\mathbf{X}_0 + \delta\mathbf{X}_0)$, where $\delta\mathbf{X}_0$ is assumed to be small. For certain parameter combinations, the trajectories from these two initial conditions start separating exponentially under the action of the flow. This exponential separation is the cause of the observed chaotic behavior in nonlinear deterministic systems,[3-10] and is called the *sensitive dependence on initial conditions*. For dissipative systems, a stretching in one direction has to be accompanied by a more-than-compensating contraction in other directions, so that the volume of an arbitrary droplet of initial conditions will contract with time.

The phase-space trajectories for a chaotic system asymptotically approach an attractor that is different from the three mentioned above. A chaotic attractor has a folded, layered structure with a fractional dimension (i.e., it is a fractal) and is called a strange attractor. The layered structure of a strange attractor is due to the properties of the flow in phase space described above. The systems are deterministic, so that trajectories cannot intersect in phase space. Because the attractor is bounded in phase space, two trajectories on the attractor in a chaotic regime cannot diverge forever; hence, the attractor has to "fold back" into the same region of phase space. The folding of the attractor is such that there must be a finite volume of phase space (which is not a part of the attractor) between the folds. Hence, a chaotic attractor ends up as a folded, layered structure, with local stretching (nearby trajectories diverging exponentially) and a fractional dimension that is less than the dimension of the full phase space. The determination of the fractal dimension of chaotic attractors[3,6,7,15-17]

is an interesting topic, but one that we will not discuss further here. Finally, it has been shown that the dimension of a chaotic attractor must be greater than two.[18] Thus a chaotic system must have more than 1 degree of freedom. It turns out that $1\frac{1}{2}$ degrees of freedom (three-dimensional phase space) will suffice.

There are at least three scenarios by which the regular behavior of a system changes to a chaotic behavior; each scenario has its own set of universal scaling laws. The first scenario is the period-doubling route to chaos in which the period of the solution bifurcates at certain values of a driving parameter (from a period 1 solution, to period 2, to period 4, and so on) until, at a critical value of the parameter, the solution is chaotic. The ratios of the difference between parameter values at which the bifurcations occur have been found to approach a universal value $\delta = 4.6692...$, called Feigenbaum's delta.[3–9] Two other universal routes to chaos are fairly well understood: intermittent and quasiperiodic. As an example of the intermittent route, a regular signal becomes interrupted by bursts of chaos, until, at a critical parameter value, the signal is continually chaotic.[3–9] In the quasiperiodic route,[3–9] the system approaches chaos via the breaking up of a quasiperiodic orbit (or torus attractor). Not all systems follow one of these routes and there are almost certainly other universal routes yet to be discovered. Some of the results discussed later in this article concern the period-doubling route to chaos.

III. LYAPUNOV EXPONENTS

The Lyapunov exponent is a measure of the rate of divergence (or convergence) of, initially infinitesimally separated, trajectories.[3–10,17] An attractor is chaotic if it has at least one positive Lyapunov exponent, which means nearby trajectories are diverging. An excellent discussion of Lyapunov exponents is given by Wolf (in Chap. 13 of Ref. 6).

One can define the Lyapunov exponents for an attractor by considering an initial point on the attractor in an n-dimensional phase space, with an infinitesimal hyperspherical droplet of initial conditions centered around it. Under the action of the flow, the spherical droplet will deform to a hyperellipsoid, and the ith Lyapunov exponent[17] is given by

$$\lambda_i = \lim_{\substack{t\to\infty \\ p_i(0)\to 0}} \left[\frac{1}{t}\log\left(\frac{p_i(t)}{p_i(0)}\right)\right], \tag{3}$$

where $p_i(t)$ is the length of the ith principal axis of the hyperellipsoid at time t. Either base 2 or base e may be used for the logarithm. In this article, we denote Lyapunov exponents by λ when base 2 is used, and by μ when base e is used; λ and μ being related by $2^{\lambda} = e^{\mu}$. If logarithms to base 2 are used in Eq. (3), the units of the Lyapunov exponents will be in bits/s.

Since the principal axes of the ellipsoid continuously change directions, one cannot talk of a well-defined direction for a Lyapunov exponent.[6,17] There will be an exponent for each phase-space dimension, and one can order the exponents, from largest to smallest, to form a Lyapunov exponent spectrum. It has been shown that if the trajectory does not end at a fixed point, then at least one Lyapunov exponent is equal to zero.[19] The sign of the Lyapunov exponents in the spectrum may be used to clarify the type of attractor associated with the flow. Consider, for example, a three-dimensional phase-space flow. Then all negative exponents, denoted by $(-,-,-)$, will indicate the presence of a fixed point, while $(0,-,-)$ indicates a limit cycle and $(+,0,-)$ a chaotic attractor.[3–7,17] Therefore, if we want to determine whether a system is chaotic, we need only determine whether the largest Lyapunov exponent is positive. A positive Lyapunov exponent λ measures the rate of separation of trajectories, with the predictive power of the initial condition being lost at the rate of λ bits/s.

Therefore, any initial error to a chaotic solution rapidly increases. When doing a numerical simulation of a physical model exhibiting chaos, errors due to both the numerical integration technique, as well as those due to the finite representation of real numbers in a computer, will be expected to affect the solution. How sure are we, then, that the phase trajectory is correct? For dissipative systems, the negative Lyapunov exponents stabilize the solution and ensure that we end up on the attractor, but the error in the position on the attractor may be as large as the attractor itself. All that one can say is that the solution is on the attractor and that there is an initial condition, near the one from which we started, for which the deterministic solution would agree with our solution.[20] One can compare the results of different numerical methods to ensure that the same attractor is attained for the same initial conditions and parameter values.

A. Local linearization of the equations

The determination of the Lyapunov exponents is achieved by *linearizing* the equations defining the flow in the neighborhood of a point on a trajectory. Without loss of generalization, let us limit the discussion to a three-dimensional phase space. Let $\mathbf{X} = (x, y, z)$ be a vector describing the coordinates of a point that generates a trajectory in phase space under the action of the flow defined by Eq. (1). Suppose we have two initial points, $\mathbf{X}_0 = (x, y, z)$ and $\mathbf{X}_0 + \mathbf{a} = (x + \delta x, y + \delta y, z + \delta z)$, which are separated by the infinitesimal amount, $\mathbf{a}$. We want to measure the rate of separation of the two trajectories by obtaining the equation for the evolution of the difference, $\mathbf{a}$.

If we consider the x component of $\mathbf{a}$ and omit L in the notation, then

$$\frac{d(\delta x)}{dt} = \frac{d(x+\delta x)}{dt} - \frac{dx}{dt}$$
$$= G_1(x+\delta x, y+\delta y, z+\delta z) - G_1(x, y, z).$$

This is equivalent to the first (linear) terms of a multivariate Taylor series expansion

$$\frac{d(\delta x)}{dt} = \frac{\partial G_1}{\partial x}\delta x + \frac{\partial G_1}{\partial y}\delta y + \frac{\partial G_1}{\partial z}\delta z, \tag{4}$$

with the partial derivatives being evaluated at (x, y, z). Similarly, one can obtain the equivalent expressions for the other components. Thus the expression for the evolution of the difference $\mathbf{a}$ is $d\mathbf{a}/dt = \tilde{M}(x, y, z)\mathbf{a}$, where $\tilde{M}$ is the 3×3 Jacobian matrix of the generalized velocity vector field $\mathbf{G}(\mathbf{X})$ evaluated at (x, y, z), obtained as shown above. The Lyapunov exponents are related to the eigenvalues of this matrix.[3]

In special situations, analytical methods can be used to obtain the Lyapunov spectra, while numerical methods must be used in general. When we have a stationary solution given by $d\mathbf{X}/dt = \mathbf{G}(\mathbf{X}) = \mathbf{0}$, the Jacobian matrix is

then time-independent, and we can analytically obtain the (possibly complex) eigenvalues, from which the Lyapunov exponents can be calculated. In the general case, there is no stationary solution, and the linearized equations $d\mathbf{a}/dt = \tilde{M}(x,y,z)\,\mathbf{a}$ must be solved numerically along with the numerical solution of $d\mathbf{X}/dt = \mathbf{G}(\mathbf{X})$, which gives the central trajectory $\mathbf{X} = (x, y, z)$.

B. Determination of the Lyapunov exponent spectra when there is a stationary solution

As a specific example, consider the Duffing equation (circa 1918), which describes the motion of a periodically forced damped unit mass in a two-well potential, symmetric about the origin. The system is modeled by the following set of dimensionless coupled equations:

$$\begin{aligned}\frac{dx}{dt} &= y = G_1(x,y,z),\\ \frac{dy}{dt} &= x(1-x^2) - cy + F\cos(z) = G_2(x,y,z), \qquad (5)\\ \frac{dz}{dt} &= \omega = G_3(x,y,z),\end{aligned}$$

where c is the damping term and F is the amplitude of the forcing term. This system has a phase space of three dimensions: x is the position (y the velocity) of the particle, and z is the phase of the forcing function. The form of the potential function $U(x)$ can be obtained by recognizing that the second equation is Newton's second law for the system, with the damping and periodic driving force added. Therefore, since $F_x = -dU/dX$, we find that $U(x) = -(x^2/2)[1 - x^2/2]$ (see Fig. 1). Note that the phase space of Eq. (5) has three dimensions, corresponding to $1\frac{1}{2}$ degrees of freedom. The free (undriven) system has 1 degree of freedom (two-dimensional phase space) and hence cannot be chaotic. When a periodic driving force, $F\cos(\omega t)$, is added, we can add one dimension to the phase space, $z = \omega t$, thereby maintaining an autonomous (time-independent) velocity vector field, $\mathbf{G}$. The periodic driving force, therefore, effectively adds $\frac{1}{2}$ degree of freedom to the system, making a total of $1\frac{1}{2}$ degrees of freedom, and chaos possible.

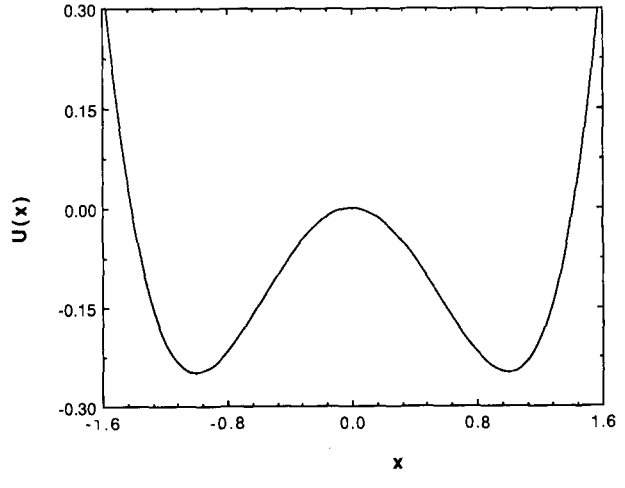

Fig. 1. A Duffing two-well oscillator potential $U(x)$. The two stable equilibrium points are at $x = \pm 1$ and the unstable equilibrium point is at $x = 0$. A particle in this potential experiencing both damping proportional to the velocity and a periodic driving force will behave chaotically for certain values of the driving force and damping constant.

When finding the Lyapunov exponents in this model, the z component plays a special role since it is always increasing linearly and therefore cannot possibly be the cause of any exponential separation. Indeed, when one uses Eq. (5) to obtain the Jacobian matrix $\tilde{M}$ for the system, it is seen that $d(\delta z)/dt$ is always equal to 0, meaning that we always have at least one 0 Lyapunov exponent for the Duffing equation:

$$\tilde{M} = \begin{bmatrix} \frac{\partial G_1}{\partial x} & \frac{\partial G_1}{\partial y} & \frac{\partial G_1}{\partial z} \\ \frac{\partial G_2}{\partial x} & \frac{\partial G_2}{\partial y} & \frac{\partial G_2}{\partial z} \\ \frac{\partial G_3}{\partial x} & \frac{\partial G_3}{\partial y} & \frac{\partial G_3}{\partial z} \end{bmatrix} = \begin{bmatrix} 0 & 1 & 0 \\ 1-3x^2 & -c & -F\sin z \\ 0 & 0 & 0 \end{bmatrix}.$$

Stationary solutions occur only if there is both no forcing ($F = 0$) and some damping ($c > 0$) present in the system, which is what we shall assume for the remainder of this subsection. The variables (x, y) have three stationary solutions: $y = 0$ at $x = 0$ or $+1$ or -1. From Fig. 1, we see that $x = 0$ is a position of unstable equilibrium while the other two are stable. Let us now consider the case where the mass settles into one of the potential wells ($x = \pm 1$). Since both the last row and last column of the Jacobian matrix consist entirely of zeros, we can ignore them and instead solve the system of equations for the corresponding 2×2 matrix system, $d\mathbf{b}/dt = \tilde{\mathbf{N}}\mathbf{b}$, $\mathbf{b}$ being the vector $(\delta x, \delta y)$:

$$\begin{bmatrix} d(\delta x)/dt \\ d(\delta y)/dt \end{bmatrix} = \begin{bmatrix} 0 & 1 \\ -2 & -c \end{bmatrix}\begin{bmatrix} \delta x \\ \delta y \end{bmatrix} \quad (F_0 = 0, \quad c > 0).$$

$\tilde{N}$ has two eigenvalues, μ_1 and μ_2, where $\mu_1 = [-c + (c^2 - 8)^{1/2}]/2$, and $\mu_2 = [-c - (c^2 - 8)^{1/2}]/2$. The general solution for $\delta x(t)$ and $\delta y(t)$ are linear combinations of $e^{\mu_1 t}$ and $e^{\mu_2 t}$.

There are three cases to consider: (a) $c^2 - 8 > 0$; μ_1 and μ_2 are distinct, negative, and real, and the three Lyapunov exponents are distinct $(0, \mu_1, \mu_2)$; (b) $c^2 - 8 = 0$; μ_1 and μ_2 are identical, negative, and real, so that two Lyapunov exponents are identical (the third will be 0); (c) $c^2 - 8 < 0$; μ_1 and μ_2 are complex conjugates, $a \pm ib$. The imaginary part leads to an oscillatory term (by Euler's formula), which does not contribute to the time-average separation when determining the Lyapunov exponent [see Eq. (3)]. Thus only the real part ($a = -c/2$) determines the Lyapunov exponent. Therefore, again, two Lyapunov exponents are identical and negative, with the third being zero. In more conventional terms, case (a) is *overdamped*; case (b) corresponds to *critical damping*; and case (c) is *underdamped*.

For later comparison with numerical experiments, consider the specific case $c = 0.5$. Then $c^2 - 8 < 0$, giving $\mu_1 = \mu_2 = \mu = -c/2 = -0.25$. These eigenvalues μ determine the separation rate in terms of the natural logarithm (i.e., $A = A_o e^{\mu t}$, A_o being the initial separation). Using base 2 gives the Lyapunov exponent $\lambda = \mu/\ln(2) = -0.25/\ln(2)$ bits/s $= -0.3607$ bits/s for this case. The complete Lyapunov exponent spectra is

therefore given by $(0, -0.3607, -0.3607)$ bits/s. We compare the results of numerical experiments with this analytic result in Sec. IV.

Summarizing the analytic results for $F=0$, we have found two stationary point attractors at $x=\pm 1$, $y=0$, with one Lyapunov exponent always zero, and the other two exponents negative and equal (underdamped) until $c=\sqrt{8}$ (critical damping). If c is increased beyond this value (overdamping), one of the exponents increases with c but remains less than 0, and the other continually decreases (as $c\rightarrow\infty$). Thus there is no chaos (i.e., no attractor with a positive Lyapunov exponent) for $F=0$, $0<c<\infty$.

C. Numerical determination of Lyapunov exponents

In general, it is impossible to integrate analytically the linearized equations, and numerical methods must be used. The Lyapunov exponents can be determined from the following numerical technique proposed by Wolf *et al.*[17] For a system described by an n-dimensional phase space, the initial condition is taken as the center of n orthogonal vectors initially of unit length, which represent the principal axes of an infinitesimal n hypersphere. The Lyapunov exponents are determined from the growth rate of the n principal axes under the action of the flow. The phase space or (fiducial[6,17]) trajectory leaving the initial condition is determined by integrating the nonlinear equations defining the flow. Simultaneously, one can determine the tangential trajectories of the n unit vectors by integrating the local linearized equations along with the fiducial trajectory.[6,17] Thus determination of the Lyapunov exponent spectra for a system modeled by an n-dimensional phase space requires the simultaneous numerical integration of $(1+n)n$ first-order differential equations. As the fiducial trajectory moves with the flow, the surface of the infinitesimal hypersphere deforms as each initial unit vector changes magnitude and direction in accordance with the local linearized equations. However, two problems arise during the calculation. First, if the linearized vectors are allowed to grow too large or too small, computer number representation problems occur. Second, all the linearized vectors tend to move toward the direction of most rapid growth. These two problems are overcome by repeated Gram Schmidt Reorthonormalization (GSR).[6,17] The GSR must be done fairly frequently; e.g., in the case of the Duffing oscillator model, the GSR is applied once every forcing period. By keeping track of the sizes of each vector before every GSR, the total length L_i of each orthogonal vector is known at any time t and, thus, we can use $\lambda_i(t)=(\log_2 L_i)/t$ to get an estimate of the Lyapunov spectrum averaged over the finite time interval, t. As t increases, the values of $\lambda_i(t)$ will approach the correct Lyapunov spectrum for the attractor.

IV. RESULTS AND DISCUSSION OF THE NUMERICAL EXPERIMENTS

The Duffing equations [Eq. (5)] describe the motion of a particle in a two-well potential (see Fig. 1) with damping and a periodic driving force. In the dimensionless units used, the natural frequency of small oscillations at the bottom of either well is $\omega_o=\sqrt{2}$. The Duffing equations are found to model a number of physical systems.[7]

The results reported here were obtained using the program DUFFING, which is a part of "The Chaotic Dynamics Workbench" (CDW) software[21] developed by one of the authors (RWR). The program was written in TURBO PASCAL version 3, for an IBM PC/XT/AT or compatible with 512 K of memory, an 8087 or 80287 math coprocessor, and CGA graphics. A fourth-order Runge–Kutta method is used to integrate the set of differential equations [Eq. (5)]. The CDW provides several features useful for both qualitative and quantitative studies on nonlinear systems. A very interactive environment is provided where the system parameters (such as F, c, and ω) can be changed while the integration is proceeding. Thus the effect on the trajectory in phase space, caused by changing the parameters, can be viewed immediately. Graphics capabilities include panning and zooming projections of the trajectory in phase space, a choice between viewing the trajectory in phase space or up to 20 different Poincaré sections[3–7] (intersections of a trajectory with hyperplanes in phase space). The CDW also allows the calculation of the Lyapunov exponent spectra using the Wolf *et al.*[17] method described in Sec. III C. The particular microcomputer used for most of this work was an IBM-AT-compatible, with a 80287 math coprocessor, running at 8 MHz.

The program was used to investigate interactively the general behavior of the system described by Eq. (5) for different values of the parameters F, c, and ω. We report below the results of a particular systematic study in the parameter space. The damping and driving frequency were fixed at $c=0.5$ and $\omega=1.0$ and the response of the system was studied as the amplitude of the driving force F was varied over a range from 0 to about 1.0. The general behavior was investigated using an integration step size such that there were 25 time steps per drive period. The global behavior observed is described below.

For $F=0$, the mass settles into the bottom of one of the potential wells at either $x=\pm 1.0$; which well depends on the initial conditions. As F is increased from zero, the mass (originally at the bottom of one well) oscillates near the bottom of the well with a single period equal to the drive period. A projection of a period-1 attractor onto the position–velocity plane of phase space is shown in Fig. 2(a). The amplitude of the period-1 oscillation increases smoothly as F is increased until F reaches about 0.321, where there is a sudden jump to a larger response amplitude. Amplitude jumps (and the associated hysteresis) are common in nonlinear oscillators.[22] Hysteresis in the response, as a function of F, is observed over a range: $0.309<F<0.321$. After the response jumps to a larger period-1 oscillation as F is increased above 0.321, a decrease in F results in a smooth decrease in amplitude until F reaches 0.309, where the amplitude jumps back down to the amplitude observed while increasing F from 0. Thus, in the range $0.309<F<0.321$, there are two period-1 attractors in *each* well. Which orbit the system settles into depends on the initial conditions.

Further increasing F beyond 0.321 leads to a series of period-doubling transitions (or bifurcations). For example, at $F=F_1\approx 0.344$, the attractor changes from an orbit that closes after one drive period to an orbit that closes after two drive periods. This is a period-2 attractor [see Fig. 2(b)]. At $F=F_2\approx 0.355$, the orbit bifurcates again into a period-4 attractor. This period doubling continues with a bifurcation to a period-2^n attractor occurring at $F=F_n$. The range $F_n<F<F_{n+1}$ for the period-2^n attractor gets smaller in geometric progression as n increases. This is an example of the period-doubling route to chaos. Careful determination of the bifurcation points

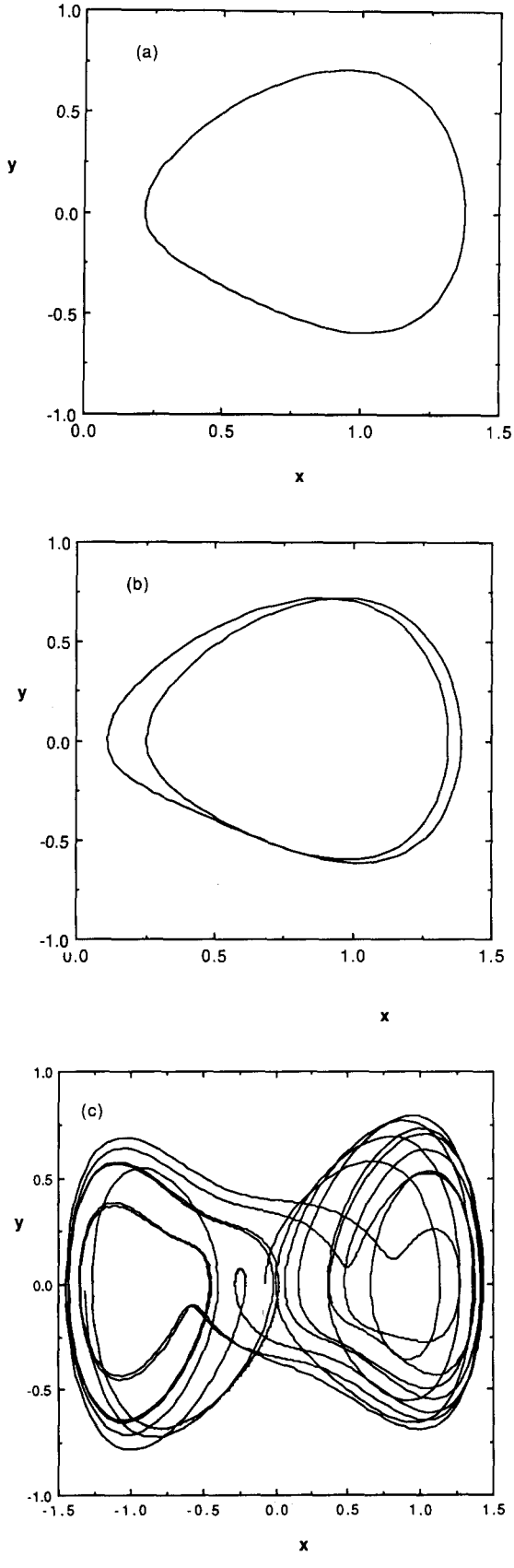

Fig. 2. The orbit of the Duffing oscillator in phase space where y corresponds to a dimensionless velocity and x, a dimensionless position. The three plots are for the same damping constant $c = 0.5$ and drive frequency $\omega = 1.0$, but have different values for the driving force amplitude F. (a) A period-1 orbit about the $x = 1$ equilibrium point (see Fig. 1) occurs when $F = 0.325$. (b) The driving force amplitude has increased to $F = 0.348\,75$, causing the bifurcation to a period-2 orbit. (c) When F becomes 0.420, the orbit is chaotic.

gave $F_1 = 0.343\,57 \pm (2)$; $F_2 = 0.355\,06 \pm (1)$; $F_3 = 0.357\,85(\pm 1)$; and $F_4 = 0.358\,46(\pm 1)$, where the error reported represents the uncertainty in the last digit. The period-doubling route to chaos should exhibit universal scaling laws.[3-9] For example,

$$\delta = \lim_{n\to\infty} \delta_n = 4.6692...,$$

where $\delta_n = (F_n - F_{n-1})/(F_{n+1} - F_n)$. Our data are consistent with this prediction; e.g., we have $\delta_3 = (F_3 - F_2)/(F_4 - F_3) = 4.57 \pm 0.2$. From δ and the measured F_n, we can estimate that the onset of chaotic orbits should occur at $F_\infty = 0.3586$ and this is also in agreement with the numerical experiments.

For $F \geqslant 0.36$, the observed orbits are generally not periodic. This is the chaotic regime. For $F \leqslant 0.386$, the chaotic orbits remain trapped in one well, but for larger F, the orbit visits both wells [see Fig. 2(c)]. Within the chaotic region, there are narrow ranges of F for which periodic orbits exist. For example, at $F = 0.455$, a period-5 orbit exists that circles $x = +1$ twice, then goes over to the other well and circles $x = -1$ twice. Finally, for $0.83 \leqslant F \leqslant 1.0$, all attractors seem to be large period-1 orbits circling $x = 0$ once each cycle. The *qualitative* behavior described above could be verified by anyone in 10–20 min. with a suitable personal computer and the DUFFING program.

A survey of the Lyapunov spectra over the same parameter range was undertaken. The rate of convergence of the Lyapunov exponents calculated using the Wolf *et al.*[17] algorithm described in Sec. II C is shown in Fig. 3. The calculated value of the most positive Lyapunov exponent is plotted as a function of the total averaging time, measured in units of the drive period. Reasonably good convergence is attained after about 500 drive periods. As a check on the numerical methods used, the Lyapunov spectra were numerically calculated at $F = 0$, where an analytical solution

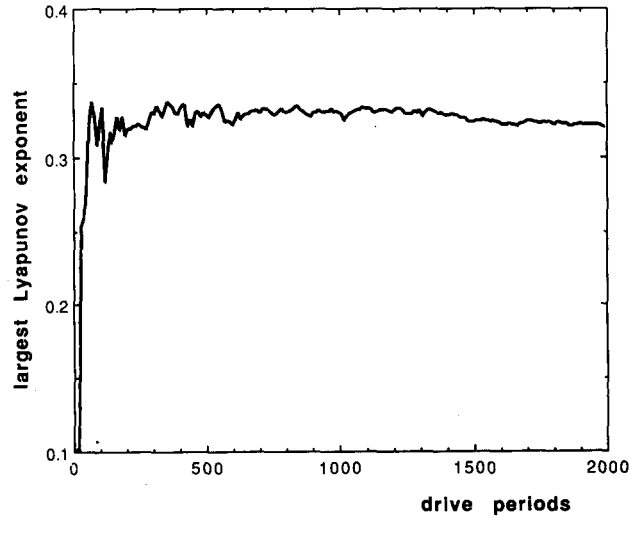

Fig. 3. The time for the system to relax to its steady-state solution depends upon the model and the parameter values. This plot shows the largest Lyapunov exponent, in units of bits per drive period, for the Duffing oscillator when the damping constant c is 0.5, the driving force amplitude F is 0.47, and the drive frequency ω is 1.0. This is a situation where the behavior is chaotic as indicated by the positive values of this Lyapunov exponent. Consistent values for the exponents are typically obtained after 500 drive periods. One drive period equals $(2\pi/\omega)$ s.

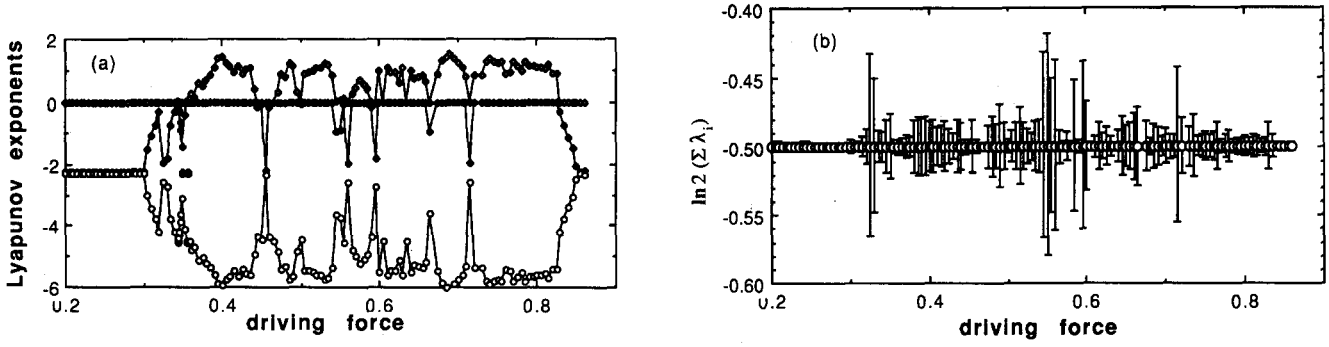

Fig. 4. The values of the three λ Lyapunov exponents, in units of bits per drive period, describing the Duffing oscillator are plotted in (a) as a function of the driving force amplitude F, when the damping constant $c = 0.5$ and the drive frequency $\omega = 1.0$. Different symbols are used for the three Lyapunov exponents, which are ordered from largest to smallest. At low values of F, the system is periodic since the largest Lyapunov exponent is zero. The system follows a period-doubling route to chaos that occurs at $F_\infty \approx 0.36$, when the largest Lyapunov exponent becomes larger than 0. The system remains typically chaotic until the driving force gets very large ($F > 0.84$) except for windows of periodicity, which occur throughout the chaotic region. Plot (b) illustrates the constant value of the sum of the Lyapunov exponents (in units of bits per second) at the theoretically expected value of $-c = -0.5$. The error bars are from the standard deviation of the individual exponents over the last 100 drive periods (see Fig. 3). The largest errors occur close to the windows of periodicity, which are very sensitive to the parameter choice. Clearly the error in the sum is always much less than the error in the estimate of the individual exponents. This is discussed further in the text.

may be obtained as described in Sec. II B. For $F = 0$, the system was started with initial conditions: (position) $x = 1.0$ and (velocity) $y = -1.0$. After a transient time, the mass settles into the bottom of the well at $x = 1.0$. At this point, the Lyapunov exponent spectrum calculation is started and, after 200 drive periods, the Lyapunov spectra calculated by the program are (0.0, -0.3603 bits/s, -0.3608 bits/s). (Note: for $\omega = 1$, the reduced units are such that one drive period is 2π s.) This compares very favorably with the analytical result obtained in Sec. II B: (0.0, -0.3607 bits/s, -0.3607 bits/s).

To facilitate the Lyapunov exponent data collection, the program was modified such that the Lyapunov exponents calculated for 500 drive periods were saved in a file. Then the value of the parameter was altered and the calculation restarted from the same initial condition, saving, in a new file, the Lyapunov exponents calculated from the new set of parameters. After the Lyapunov exponents had been saved for the desired number of parameter values, the data files were analyzed. The initial few estimates for the Lyapunov exponents calculated for each set of parameter values were discarded, since they represent initial contraction and stretching rates associated with transients as the trajectory approached the attractor. The remaining estimates for the Lyapunov exponents were then averaged, and the standard deviations found, for each set of parameter values.

Figure 4(a) and (b) shows the results of one such experiment where F was varied from 0.200 to 0.850 in steps of 0.005. The values of c and ω were held constant at 0.5 and 1.0, respectively; the integration time-step size was 0.1256 (50 steps per drive period); and the initial conditions were (position) $x = +1.0$, (velocity) $y = -1.0$, and (phase of the drive) $z = 0.0$. Figure 4(a) shows the individual Lyapunov exponents as a function of F. The results show the nonzero Lyapunov exponents are negative for $F \leqslant 0.36$ where the attractors are periodic. As discussed in Sec. III, negative Lyapunov exponents indicate stable predictable behavior. However, for $F > 0.36$, the largest Lyapunov exponent is often positive, indicating a sensitive dependence on initial conditions and a chaotic attractor. For example, a typical value calculated for the largest Lyapunov exponent may be about 1 bit per drive period. This means the distance between two nearby trajectories will double after each successive drive period. Thus, if we use 64 bit numbers in the calculation, the solution is no longer correctly associated with the particular initial condition used after only 64 drive periods. Figure 4(a) also shows windows in $F > 0.36$ where no Lyapunov exponent is positive. These correspond to values of F where the orbits are periodic, e.g., the period-5 orbit mentioned above at $F = 0.455$.

Figure 4(b) shows the sum of the calculated Lyapunov exponents, multiplied by $\ln(2)$, and plotted against F. We see that this sum is constant and equal to $-c$, where c is the damping. In fact, as the points in relation to the error bars show, the sum of the Lyapunov exponents is constant to a much higher accuracy than the fluctuations of the individual Lyapunov exponents would indicate. This is an example of an important sum rule, satisfied by the Lyapunov exponents, which can be understood by the geometry of the flow of points in phase space. The Lyapunov exponents measure the rate of stretching (or contraction) of the principal axes of an n-dimensional infinitesimal hypersphere centered on a point moving along a central fiducial trajectory. When we multiply the growth rate of all of the n-axis elements together (i.e., sum the Lyapunov exponents), we determine the rate of *volume* expansion of the linearized flow surrounding a point moving along the fiducial trajectory in phase space. (Of course, the sum of the Lyapunov exponents must be negative in our case because phase-space volumes contract for dissipative flows.) Equation (2) shows that the rate of change of an infinitesimal volume element in phase space under the action of the flow is given by the generalized divergence (or Lie derivative) of the generalized velocity vector field. The sum of the Lyapunov exponents (base e) should, therefore, be equal to the generalized divergence of the flow,

$$\sum_{i=1}^{n} \frac{\partial G_i}{\partial x_i} = \ln(2) \sum_{i=1}^{n} \lambda_i. \tag{6}$$

This result can be used as a check on the numerical calculation of the Lyapunov exponent spectrum.

From Eq. (5), the generalized divergence of a flow modeled by the Duffing equations is given by $-c$ (i.e.,

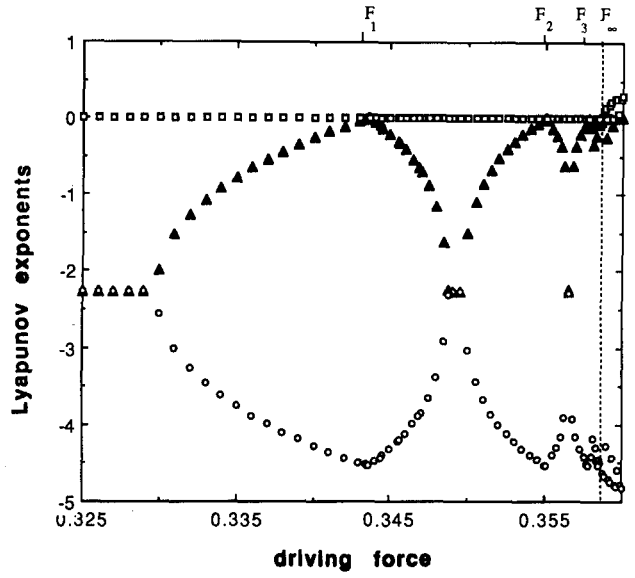

Fig. 5. More careful calculation of the Lyapunov exponents for the region in Fig. 4(a), which shows the period-doubling route to chaos by the Duffing oscillator. Bifurcation occurs when the two largest Lyapunov exponents are both equal to zero at the values of the driving-force amplitude F_n, which is indicated for $n < 4$. For $F > F_\infty$, chaotic orbits exist. The most stable periodic orbits exist when the two negative Lyapunov exponents are equal, as discussed in the text.

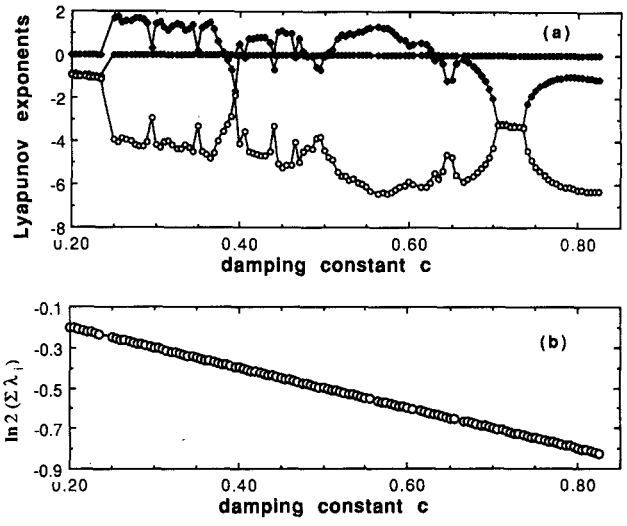

Fig. 6. (a) The values of the λ Lyapunov exponents, in units of bits per drive period, describing the Duffing oscillator when the damping constant c is varied and the driving force $F = 0.45$. The value of ω and the meaning of the symbols are the same as in Fig. 4. The obvious symmetry in (a) is due to the sum of the Lyapunov exponents being a constant that is equal to $-c$, as shown in (b), where the Lyapunov exponents now have units of bits per second.

$dV/dt = -cV$). For Fig. 4, $c = 0.5$, and the sum of the Lyapunov exponents (base e) is also -0.5, and independent of F, as expected. The interesting result that the sum of the calculated Lyapunov exponents fluctuates much less than the individual exponents suggests that the method of Wolf *et al.*[17] does a very good job of measuring the local contraction of the flow in phase space. The local contraction is constant and equal to $-c$ everywhere in phase space for the Duffing oscillator. The individual Lyapunov exponents are not constant everywhere in phase space and, hence, their time average over a trajectory will fluctuate, especially for short time averages [see Eq. (3)].

Figure 5 shows a more careful study of the period-doubling region shown in Fig. 4(a) for $F \leqslant 0.36$. For these data, we waited 500 drive periods after changing F to a new value so that any resulting transients had disappeared before we started to calculate the Lyapunov spectrum. Then the calculated Lyapunov spectrum was averaged over at least 2000 drive periods and the last value calculated was plotted. The structured behavior of the Lyapunov spectra shown in this plot as the system follows the period-doubling route to chaos is not well known.[23] Two interesting features are visible. First, we see that the second largest Lyapunov exponent goes to zero at each bifurcation point where $F = F_n$. Physically, a negative Lyapunov exponent approaching zero represents a weakening in the stability of the trajectory, since a small displacement from the attractor will take a longer and longer time to return. Second, we note that there appears to be a short range in F where the two negative Lyapunov exponents are equal for each period-n orbit. Interpreted physically, these are the "most stable" period-n orbits in the sense that any perturbed orbit will return to the periodic attractor most rapidly for F in the most stable range. These orbits correspond to the "superstable" orbits that appear during period doubling in one-dimensional maps where the (only) Lyapunov exponent goes to negative infinity.

We now return to the sum rule given by Eq. (6). Figure 6 shows results from another run of the Duffing model, in which F and ω were held constant at 0.45 and 1.00, respectively, while c varied from 0.2 to 0.825 in steps of 0.005. The integration step size and initial conditions were the same as for the results shown in Fig. 4. Figure 6(a) shows all three individual Lyapunov exponents plotted against c, while Fig. 6(b) shows the sum of the exponents multiplied by $\ln(2)$ plotted against c. One sees that the sum of the exponents is always equal to $-c$, as expected. One interesting feature of Fig. 6(a) is that the two negative exponents come together for a small range $0.70 \leqslant c \leqslant 0.74$, and then separate again. This is similar to the most stable orbits mentioned above. In this region, while the damping is monotonically increased, the system apparently goes from overdamped to underdamped and then back to overdamped again.

The same investigation of the sum rule was carried out for two other models, the Lorenz system[24] and the Shaw–Van der Pol oscillator.[25] The results for the Lorenz system were as expected, and are not presented here: Namely, the sum of the Lyapunov exponents was independent of the Rayleigh number R, but dependent on the other two parameters σ and β, in accordance with the Lie derivative for the system ($dV/dt = -[\sigma + \beta + 1]V$).

However, the Shaw–Van der Pol oscillator presents a different situation. The equations modeling this system[24] are

$$\frac{dx}{dt} = y + F\sin(z),$$

$$\frac{dy}{dt} = -\frac{[x + y(3Bx^2 - A)]}{C},$$

$$\frac{dz}{dt} = \omega.$$

The Lie derivative depends on the parameters (as is the case for the Duffing and Lorenz systems) *and* also depends on the variable x, as x^2. When studying this system, the

parameters A, B, C, and ω were held constant, while F was varied. A time series of the variable x was saved for each set of parameter values. The value of $\langle x^2 \rangle \equiv (x^2$ averaged over the trajectory) and its standard deviation were calculated. Also, the Lyapunov exponent spectra were saved. The preliminary results indicate that the sum of the Lyapunov exponents is equal to the *average* divergence of the flow (as suggested by Wolf in Ref. 6) given, in this case, by $A/C - 3B\langle x^2 \rangle / C$.

V. CONCLUSIONS

The numerical experiments reported on the Duffing two-well oscillator show a variety of the behaviors now expected in nonlinear systems. The period-doubling route to chaos was observed in this system and shown to be in agreement with a universal scaling law. The calculated Lyapunov exponent spectra show that a positive Lyapunov exponent is associated with nonperiodic behavior that appears to be chaotic. For periodic orbits, all Lyapunov exponents are nonpositive. Interesting behavior of the Lyapunov exponents was observed along the period-doubling approach to chaos. One negative Lyapunov exponent goes to zero at the point where the orbit bifurcates to double its period. Also, we found a small range of F where the most stable period-2^n orbits exist for each n where the two negative Lyapunov exponents are equal. Finally, we verified the Lyapunov sum rule [Eq. (6)] for the Duffing oscillator where the generalized divergence of the phase-space flow is constant. In addition, preliminary results on the Shaw–Van der Pol oscillator suggest that when the generalized divergence in Eq. (6) is not constant, but contains a functional dependence on the phase-space coordinates $f(x_i)$, the sum of the Lyapunov exponents is equal to the generalized divergence of the flow *averaged* over the attractor.

Perhaps the most significant conclusion is that we have demonstrated that nonlinear dynamics and the new field of chaos is very appropriate for introduction at the undergraduate level. Very simple nonlinear systems are rich with unexpected and interesting behavior that can be studied with a good interactive simulation on a microcomputer. The new techniques used in studying nonlinear systems, such as the Lyapunov exponent spectra discussed in detail here (and Poincaré sections of attractors in phase space and their fractional dimension not discussed here for lack of space), are very nicely introduced to students through interactive simulations and numerical experiments that can be performed on relatively inexpensive microcomputers with software such as CDW[21] used in this work.

ACKNOWLEDGMENTS

One of us (RWR) wishes to thank his colleagues at Ohio University—especially Earle Hunt and Sergio Ulloa—for many discussions on the physical and mathematical ideas used to describe chaotic systems. RWR also thanks several undergraduate and graduate students for testing, commenting, and otherwise assisting in the development of the CDW software. RWR received partial support from an Ohio University Academic Challenge Grant. DTJ received partial support by the National Science Foundation under Grant No. CHE87-22034.

[a] Present address: Department of Physics and Astronomy, University of Maryland, College Park, MD 20742.

[1] Tien-Yien Li and James A. Yorke, "Period three implies chaos," Am. Math. Mon. **82**, 985–992 (1975).

[2] James Gleick, *Chaos: Making a New Science* (Viking–Penguin, New York, 1987). Reviewed by James Glazier and Gemunu Gunaratne, Phys. Today **41** (2), 79 (1988).

[3] H. G. Schuster, *Deterministic Chaos* (Physik-Verlag, Weinheim, Federal Republic of Germany, 1984).

[4] P. Berge, Y. Pomeau, and C. Vidal, *Order within Chaos* (Wiley, New York, 1984). Good introduction understandable by physics undergraduates.

[5] J. M. T. Thompson and H. B. Stewart, *Nonlinear Dynamics and Chaos* (Wiley, New York, 1986).

[6] *Chaos*, edited by Arun V. Holden (Princeton U.P., Princeton, NJ, 1986).

[7] F. C. Moon, *Chaotic Vibrations* (Wiley, New York, 1987). Good introduction with an emphasis on physical experiments. Recommended for physics or engineering students.

[8] Robert L. Devaney, *An Introduction to Chaotic Dynamical Systems* (Benjamin/Cummings, Menlo Park, CA, 1986). For students of a mathematical bent.

[9] *Universality in Chaos*, edited by P. Cvitanovic (Adam Hilger, Bristol, England, 1984); *Chaos*, edited by Bai-Lin Hao (World Scientific, Singapore, 1984). Reprint selections.

[10] R. Abraham and C. D. Shaw, *Dynamics: The Geometry of Behavior*, Pt. 1–4 (Aerial, Santa Cruz, CA, 1983–1988).

[11] K. Briggs, "Simple experiments in chaotic dynamics," Am. J. Phys. **55**, 1083–1089 (1987); T. M. Mello and N. B. Tufillaro, "Strange attractors of a bouncing ball," Am. J. Phys. **55**, 316–320 (1987); N. B. Tufillaro and A. M. Albano, "Chaotic dynamics of a bouncing ball," Am. J. Phys. **54**, 939–944 (1986); H. Meissner and G. Schmidt, "A simple experiment for studying the transition from order to chaos," Am. J. Phys. **54**, 800–804 (1986); and T. Mishina, T. Kohmoto, and T. Hashi, "Simple electronic circuit for the demonstration of chaotic phenomena," Am. J. Phys. **53**, 332–334 (1985).

[12] Reference 4, p. 114.

[13] A. A. Chernikov, R. Z. Sagdeev, and G. M. Zaslavsky, "Chaos: How regular can it be?" Phys. Today **41** (11), 27–35 (1988).

[14] J. P. Crutchfield, J. D. Farmer, N. H. Packard, and R. S. Shaw, "Chaos," Sci. Am. **255** (6), 38–49 (1986).

[15] J. D. Farmer, E. Ott, and J. A. Yorke, "The dimension of chaotic attractors," Physica D **7**, 153–180 (1983).

[16] D. A. Russell, J. D. Hansen, and E. Ott, "Dimension of strange attractors," Phys. Rev. Lett. **45**, 1175–1178 (1980).

[17] A. Wolf, J. B. Swift, H. L. Swinney, and J. A. Vastano, "Determining Lyapunov exponents from a time series," Physica D **16**, 285–317 (1985).

[18] For example, see Ref. 3, pp. 114–117.

[19] H. Haken, "At least one Lyapunov exponent vanishes if the trajectory of an attractor does not contain a fixed point," Phys. Lett. A **94**, 71–72 (1983).

[20] S. M. Hammel, J. A. Yorke, and C. Grebogi, "Do numerical orbits of chaotic dynamical processes represent true orbits?" J. Complexity **3**, 136–145 (1987).

[21] R. W. Rollins, *Chaotic Dynamics Workbench* (Physics Academic Software, AIP, New York, 1990); The program DUFFING is included in *Computers in Physics Instruction: Software* (The Conference on Computers in Physics Instruction, 1988, Dept. of Physics MB, North Carolina State University, Raleigh, NC 27695-8202).

[22] Ralph Baierlein, *Newtonian Dynamics* (McGraw-Hill, New York, 1983), p. 81.

[23] Jan Frøyland and Knut H. Alfsen, "Lyapunov exponent spectra for the Lorenz model," Phys. Rev. A **29**, 2928–2931 (1984).

[24] E. N. Lorenz, "Deterministic nonperiodic flow," J. Atmos. Sci. **20**, 130–141 (1963); See also Ref. 3, Appendices A and B.

[25] Reference 10, p. 136.